CHEMISTRY
A EUROPEAN JOURNAL

DOI: 10.1002/chem.200800630

Construction of Titanasiloxanes by Incorporation of Silanols to the Metal Oxide Model [{Ti(η^5-C_5Me_5)(μ-O)}$_3$(μ_3-CR)]: DFT Elucidation of the Reaction Mechanism

Jorge J. Carbó,*[b] Octavio González-del Moral,[a] Avelino Martín,[a] Miguel Mena,[a] Josep-M. Poblet,[b] and Cristina Santamaría*[a]

Dedicated to Professor Ernesto Carmona on the occasion of his 60th birthday

Abstract: A family of novel titanasiloxanes containing the structural unit {[Ti(η^5-C_5Me_5)O]$_3$} were synthesized by hydron-transfer processes involving reactions with equimolecular amounts of μ_3-alkylidyne derivatives [{Ti(η^5-C_5Me_5)(μ-O)}$_3$(μ_3-CR)] (R = H (**1**), Me (**2**)) and monosilanols, $R_3'Si(OH)$, silanediols, $R_2'Si(OH)_2$, and the silanetriol *t*BuSi(OH)$_3$. Treatment of **1** and **2** with triorganosilanols (R′ = Ph, *i*Pr) in hexane affords the new metallasiloxane derivatives [{Ti(η^5-C_5Me_5)(μ-O)}$_3$(μ-CHR)(OSiR$_3'$)] (R = H, R′ = Ph (**3**), *i*Pr (**4**); R = Me, R′ = Ph (**5**), *i*Pr (**6**)). Analogous reactions with silanediols, (R′ = Ph, *i*Pr), give the cyclic titanasiloxanes [{Ti(η^5-C_5Me_5)(μ-O)}$_3$(μ-$O_2SiR'_2$)(R)] (R = Me, R′ = Ph (**7**), *i*Pr (**8**); R = Et, R′ = Ph (**9**), *i*Pr (**10**)). Utilization of *t*BuSi(OH)$_3$ with **1** or **2** at room temperature produces the intermediate complexes [{Ti(η^5-C_5Me_5) (μ-O)}$_3$(μ-O_2Si(OH)*t*Bu)(R)] (R = Me (**11**), Et(**12**)). Further heating of solutions of **11** or **12** affords the same compound with an adamantanoid structure, [{Ti(η^5-C_5Me_5)(μ-O)}$_3$(μ-O_3Si*t*Bu)] (**13**) and methane or ethane elimination, respectively. The X-ray crystal structures of **3**, **4**, **6**, **8**, **10**, **12**, and **13** have been determined. To gain an insight into the mechanism of these reactions, DFT calculations have been performed on the incorporation of monosilanols to the model complex [{Ti(η^5-C_5H_5)(μ-O)}$_3$(μ_3-CMe)] (**2H**). The proposed mechanism consists of three steps: 1) hydron transfer from the silanol to one of the oxygen atoms of the Ti_3O_3 ring, forming a titanasiloxane; 2) intramolecular hydron migration to the alkylidyne moiety; and 3) a μ-alkylidene ligand rotation to give the final product.

Keywords: density functional calculations · hydron transfer · oxides · silicon · titanium

Introduction

The field of metallasiloxane chemistry[1] has received considerable attention for the synthesis of soluble molecular compounds capable of mimicking the role developed by transition-metal complexes anchored on silica surfaces. Such complexes have been widely used as heterogeneous catalysts in a variety of organic transformations.[2] However, concrete aspects of these processes, such as morphology or active sites control, are scarcely known. In this way, metallasiloxanes constitute model systems capable of clarifying the reaction mechanism involved in such catalytic conversions.[3]

Soluble molecular titanasiloxanes containing the Si-O-Ti moiety exhibit efficient synthetic routes and represent potential precursors of titanosilicates, which are extensively used as heterogeneous catalysts in industrial processes.[3] Cyclic and three-dimensional titanasiloxanes with an inor-

[a] O. González-del Moral, Dr. A. Martín, Dr. M. Mena, Dr. C. Santamaría
Departamento de Química Inorgánica
Universidad de Alcalá, Campus Universitario
28871 Alcalá de Henares-Madrid (Spain)
Fax: (+34) 918-854-683
E-mail: cristina.santamaria@uah.es

[b] Dr. J. J. Carbó, Prof. Dr. J.-M. Poblet
Departament de Química Física i Inorgànica
Universitat Rovira i Virgili
Campus Sescelades C/Marcel.lí Domingo, s/n
43007 Tarragona (Spain)
Fax: (+34) 977-559-563
E-mail: j.carbo@urv.cat

Supporting information for this article is available on the WWW under http://dx.doi.org/10.1002/chem.200800630 or from the author.

ganic core and an organic boundary are particularly promising as model compounds for titanium-doped zeolites.[4]

Well-defined cyclic titanasiloxanes are most commonly prepared by reaction of silanediols or their dilithium salts with titanium chlorides. Polyhedral titanasiloxanes can be obtained by condensation of silanetriols with titanium alkoxides or chlorides. However, only a few synthetic routes have been developed involving direct reactions of silanols, silanediols, or silanetriols, and titanium derivatives containing Ti–C bonds.[1a,5] Here we show how a variety of titanasiloxanes can be synthesized readily from silanols and the cyclic derivatives $[\{Ti(\eta^5\text{-}C_5Me_5)(\mu\text{-}O)\}_3(\mu_3\text{-}CR)]$ (R = H (**1**), Me (**2**)),[6] in which a μ_3-alkylidyne moiety is supported on the organometallic oxide $[Ti(\eta^5\text{-}C_5Me_5)O]_3$ and constitutes a worthy approach to metal oxide surfaces.[7]

These novel titanasiloxanes represent some of the elementary reaction steps that hydrocarbyl fragments undergo during catalytic surface reactions (alkylidyne, alkylidene, and alkyl).[8] Furthermore, a plausible formation mechanism for these species, in which the oxygen atoms of the Ti_3O_3 core exhibit a role unknown to date, is proposed on the basis of DFT calculations.

Results and Discussion

Treatment of equimolecular amounts of the trinuclear starting materials **1** and **2** and triphenylsilanol or triisopropylsilanol, R'_3SiOH (R′ = Ph, *i*Pr), in hexane at room temperature or under moderate heating (50 °C), afforded the new metallasiloxane derivatives $[\{Ti(\eta^5\text{-}C_5Me_5)(\mu\text{-}O)\}_3(\mu\text{-}CHR)(OSiR'_3)]$ (R = H, R′ = Ph (**3**), *i*Pr (**4**); R = Me, R′ = Ph (**5**), *i*Pr (**6**)) in good yields (71–95 %), as outlined in Scheme 1. The orange-reddish (**3**, **4**) or violet microcrystalline solids (**5**, **6**) proved to be stable under argon at room temperature, and soluble in saturated hydrocarbons and aromatic solvents.

Compounds **3**–**6** were characterized by NMR and IR spectroscopy, mass spectrometry, microanalysis, and in the case of **3**, **4**, and **6** their structures were elucidated by X-ray crystallography.[9] The NMR spectra of these complexes in solution display two types signals for C_5Me_5 in a 2:1 ratio, consistent with C_s symmetry, resonance signals for the μ-alkylidene group,[7] and signals corresponding to the siloxide ligand. The molecular structure of **6** is shown in Figure 1, together with a selection of bond lengths and angles. Compound **6** reveals a trinuclear species with an alkylidene group (μ-CHR) bridging two titanium atoms and a siloxide ($-OSiR_3$) ligand linked to the third titanium in the opposite side of the Ti_3O_3 unit. Curiously, the ethylidene group shows the transferred hydrogen atom in the distal region with respect to the siloxide.

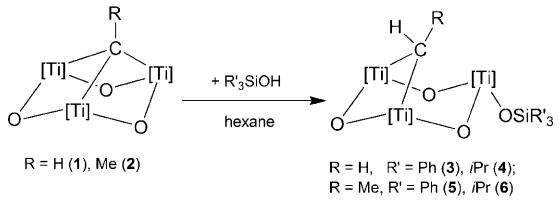

R = H (**1**), Me (**2**)

R = H, R' = Ph (**3**), *i*Pr (**4**);
R = Me, R' = Ph (**5**), *i*Pr (**6**)

Scheme 1. Synthesis of the titanasiloxanes **3**–**6**. $[Ti] = Ti(\eta^5\text{-}C_5Me_5)$.

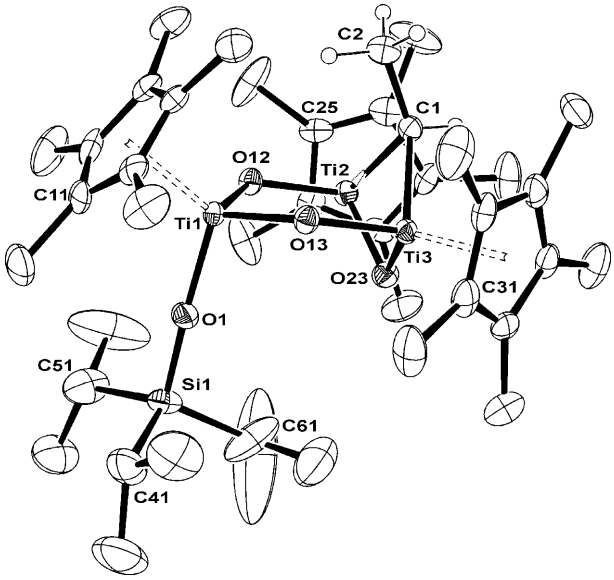

Figure 1. Molecular structure of $[\{Ti(\eta^5\text{-}C_5Me_5)(\mu\text{-}O)\}_3(\mu\text{-}CHMe)(OSi{i}Pr_3)]$ (**6**). Selected averaged bond lengths (Å) and angles (°): C1–C2 1.510(5), C1–Ti 2.128(1), Ti–O 1.854(6), Ti1···Ti 3.301(3), Ti2···Ti3 2.823(1), Si1–O1 1.642(2), Si1–C 1.909(11); Ti-C1-C2 122.4(4), Ti-C1-Ti 83.1(1), Ti2-O23-Ti3 99.4(1), Ti1-O-Ti 125.3(1), O-Ti-O 104.4(10), Ti1-O1-Si1 171.6(2), C1-Ti-O23 83.8(1), O12-Ti2-C1 100.3(1), O13-Ti3-C1 100.1(1). Hydrogen atoms, except those of the ethylidene ligand, have been omitted for clarity. Thermal ellipsoids at the 50 % probability level.

The titanium atoms present a pseudotetrahedral environment with bond lengths similar to those found in the parent compound **2**.[6a] The existence of the bridging alkylidene group makes the Ti2···Ti3 distance 0.48 Å shorter than the other two Ti1···Ti distances, and the Ti2-O23-Ti3 angle

Abstract in Spanish: *El tratamiento de los derivados μ_3-alquilidino $[\{Ti(\eta^5\text{-}C_5Me_5)(\mu\text{-}O)\}_3(\mu_3\text{-}CR)]$ (R = H (**1**), Me (**2**)) con cantidades equimoleculares de monosilanoles, $R'_3Si(OH)$, silanodioles, $R'_2Si(OH)_2$, y el silanotriol tBuSi$(OH)_3$ permite sintetizar una familia de titanosiloxanos que contienen la unidad estructural $[Ti(\eta^5\text{-}C_5Me_5)O]_3$. Con objeto de conocer el mecanismo de estas reacciones, se llevaron a cabo cálculos de DFT sobre el proceso de incorporación de monosilanoles al complejo modelo $[\{Ti(\eta^5\text{-}C_5H_5)(\mu\text{-}O)\}_3(\mu_3\text{-}CMe)]$ (**2H**). El mecanismo de reacción propuesto consta de tres etapas: 1) la transferencia de hidrón del silanol a uno de los átomos de oxígeno del anillo Ti_3O_3 con formación de una especie titanosiloxano; 2) migración intramolecular de hidrón al fragmento alquilidino; 3) la rotación directa del grupo μ-alquilideno para dar el producto final.*

(99.4(1)°) narrower than the other Ti-O-Ti angles (average 125.3(1)°), a situation comparable to those reported for [{Ti(η^5-C_5Me_5)(μ-O)}$_3$(μ-CHMe)NPh_2][7] and [{Ti(η^5-C_5Me_5)(μ-O)}$_3$(μ-CHMe)($OCMe_3$)].[10] All the Ti–O bond lengths are in the normal range (1.854(6) Å).[6] The bridging ethylidene group shows the C1 atom in a tetrahedral environment and almost equidistant with the two titanium centers (average 2.128(1) Å). The C1–C2 bond length of 1.510(5) Å is within the range for single C–C bonds.[11] The siloxide ligand, located below the Ti_3O_3 ring, shows a silicon atom in a pseudotetrahedral environment, with a Ti1-O1-Si angle (171.6(2)°) close to linearity.

To move forward with our work on these hydron-transfer processes, we investigated the reactions of **1** and **2** with substrates that contain two hydroxyl groups. Thus, the treatment of the alkylidyne species with one equivalent of silanediol in hexane at room temperature proceeds to give the cyclic titanasiloxanes [{Ti(η^5-C_5Me_5)(μ-O)}$_3$(μ-$O_2SiR'_2$)-(CH_2R)] (R = H, R′ = Ph (**7**), *i*Pr (**8**); R = Me, R′ = Ph (**9**), *i*Pr (**10**)), which are stable under argon atmosphere and soluble in most usual solvents (Scheme 2).

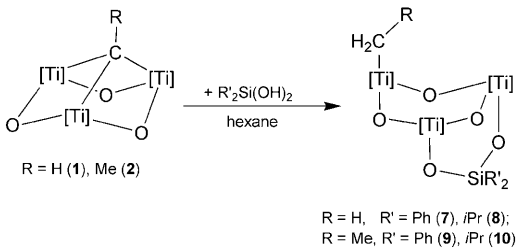

Scheme 2. Treatment of **1** and **2** with silanediols. [Ti] = Ti(η^5-C_5Me_5).

The NMR spectra (see Experimental Section) are consistent with the proposed structure and reveal the characteristic signals for methyl (**7**, **8**) or ethyl (**9**, **10**), μ-$O_2SiR'_2$ (R′ = Ph, *i*Pr) and η^5-C_5Me_5 ligands. Also, the molecular structures of **8** and **10** were elucidated by single-crystal X-ray structural analysis.[9]

The molecular structure of **10** is shown in Figure 2, together with a selection of bond lengths and angles. Complex **10** adopts a butterfly-like structure, in which two six-membered rings share an oxygen atom and two titanium metal centers. The alkyl group originating from the hydronation and the μ-O_2SiR_2 unit show a *trans* disposition with respect to the Ti_3O_3 moiety.

The Ti–C1 (2.175(5) Å) bond length is in the expected range for Ti^{IV}–C(sp^3) bond lengths[6a,7,12] and the C1–C2 bond length of 1.496(7) Å is a typical C–C single bond.[11] The shared Ti2-O23-Ti3 angle (120.8(2)°) is slightly smaller than the other two Ti-O-Ti angles (average 131.8(3)°), and is comparable with other trinuclear titanium species not bridged by chelating ligands.[12]

The scope of the above-described hydron-transfer processes was finally extended to silanetriols (see Scheme 3). The 1:1 molar ratio reaction of **1** or **2** with *tert*-butylsilanetriol at room temperature allowed us to identify the intermediate compounds [{Ti(η^5-C_5Me_5)(μ-O)}$_3$(μ-$O_2Si(OH)tBu$)(R)] (R = Me (**11**), Et (**12**)) by NMR spectroscopy and to isolate **12** as a bright yellow microcrystalline solid in good yield that is stable under argon and soluble in hydrocarbon and aromatic solvents.

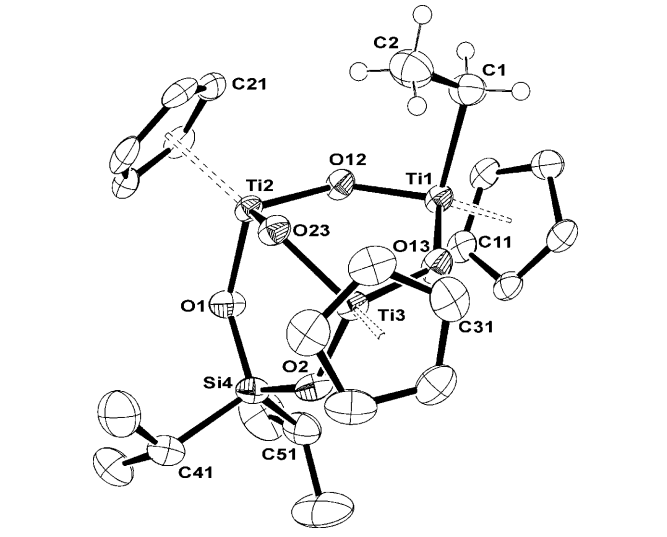

Figure 2. Molecular structure of [{Ti(η^5-C_5Me_5)(μ-O)}$_3$(μ-O_2SiiPr_2)Et] (**10**). Selected averaged bond lengths (Å) and angles (°): C1–C2 1.496(7), Ti1–C1 2.175(5), Ti–O 1.857(12), Si4–O 1.662(5), Si4–C 1.894(18); Si4-O-Ti 133.9(6), Ti2-O23-Ti3 120.8(16), Ti1-O-Ti 131.8(3), O2-Si4-O1 108.4(2), O-Si4-C 108.9(10), C41-Si4-C51 112.6(3), C1-Ti3-O 101.8(1), O-Ti-O 103(2), C2-C1-Ti1 110.9(4). Methyl groups of the pentamethylcyclopentadienyl rings and hydrogen atoms except those of the ethyl ligand have been omitted for clarity. Thermal ellipsoids at the 50% probability level.

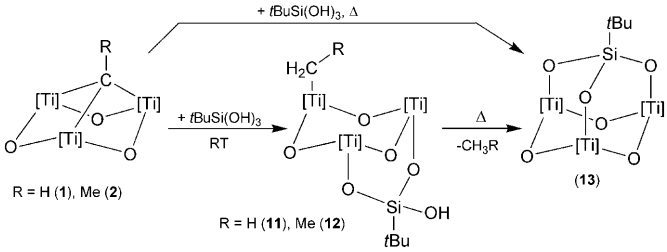

Scheme 3. Reactions of **1** and **2** with *tert*-butylsilanetriol.

The ^1H and ^{13}C spectra of **11** and **12** revealed the presence of the characteristic signals for the methyl or ethyl group, the μ-$O_2Si(OH)tBu$ fragment, and the C_5Me_5 ligands. Additionally, the molecular structure of **12** (Figure 3) was confirmed by X-ray single-structure analysis. Similarly to the geometry observed for compound **10**, complex **12** shows a butterfly-like geometry with the ethyl ligand located in the distal position with respect to that occupied by the hydroxy moiety linked to Si3. Logically, all the geometrical parameters present similar values to those found for **10**, but the lower steric requirement of the hydroxy group leads to a narrower Si-O-Ti angle (≈8°).

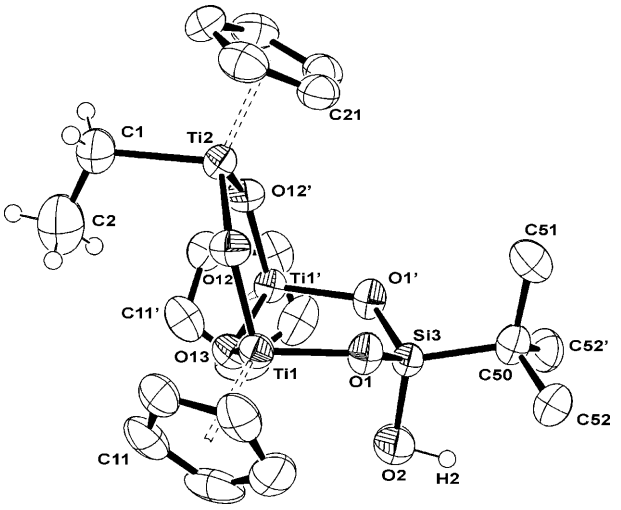

Figure 3. Molecular structure of $[\{Ti(\eta^5\text{-}C_5Me_5)(\mu\text{-}O)\}_3(\mu\text{-}O_2Si(OH)\text{-}t\text{Bu})(Et)]$ (**12**). Selected averaged bond lengths (Å) and angles (°): C1–C2 1.511(9), Ti2–C1 2.160(6), Ti–O 1.854(10), Si3–O1 1.647(2), Si3–O2 1.671(4), Si3–C50 1.881(5), Ti1···Ti2 3.367(1), Ti1···Ti1′ 3.233(1); Si3-O1-Ti1 125.6(2), Ti1-O12-Ti2 131.3(2), Ti1-O13-Ti1′ 121.8(2), O1-Si3-O1′ 108.0(2), O1-Si3-O2 109.2(2), O-Ti-O 103(3), C2-C1-Ti2 112.0(4). Methyl groups of the pentamethylcyclopentadienyl rings and hydrogen atoms except those of the ethyl and hydroxo ligands have been omitted for clarity. Thermal ellipsoids at the 50% probability level. The prime character in the labels indicates that these atoms are at equivalent position (x,-y+1/2,z).

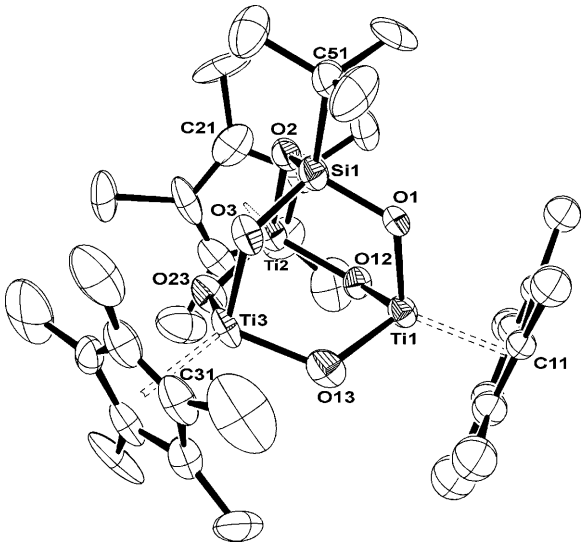

Figure 4. Molecular structure of $[\{Ti(\eta^5\text{-}C_5Me_5)(\mu\text{-}O)\}_3(\mu\text{-}O_3Si\text{t}Bu)]$ (**13**). Selected averaged bond lengths (Å) and angles (°): Ti–O 1.86(3), Si1–O 1.66(2), Si1–C51 1.888(4), Ti···Ti 3.244(14), Ti···Si1 3.074(2); Si1-O-Ti 121(2), Ti-O-Ti 122.2(9), O-Si1-O 107.8(10), O-Ti-O 100.8(8). Thermal ellipsoids at the 50% probability level.

Thermal treatment of **1** and **2** with one equivalent of *tert*-butylsilanetriol or further heating of solutions of **11** and **12** allowed us to obtain the same compound with an adamantane-like structure $[\{Ti(\eta^5\text{-}C_5Me_5)(\mu\text{-}O)\}_3(\mu\text{-}O_3Si\text{t}Bu)]$ (**13**), with methane or ethane elimination, respectively. Complex **13** is obtained in almost quantitative yields as a yellow microcrystalline solid (Scheme 3). In the ^1H and ^{13}C NMR spectra of this product, it is worth noting the single set of signals corresponding to the $\eta^5\text{-}C_5Me_5$ ligands, indicating their equivalence. The new complex retains the C_{3v} symmetry of the starting materials **1** and **2**.

Single crystals of **13**, suitable for X-ray diffraction analysis, were grown from hexane at −20 °C. The analysis (Figure 4) displays a molecule with an adamantane-type structure $[Ti_3SiO_6]$. The geometry of the cage in **13** resembles the core structure found in $[\{Ti(\eta^5\text{-}C_5Me_5)(\mu\text{-}O)\}_3(\mu\text{-}O_3SiR')]$ $(R' = (2,6\text{-}i\text{Pr}_2C_6H_3)NSiMe_3)$[5a] and $[\{Ti(\eta^5\text{-}C_5Me_5)\}_4(\mu\text{-}O)_6]$.[13]

It can be seen that the geometrical parameters in **13** are very similar to those found for complexes **10** and **12**. The only noticeable differences are found in the values of the Si1-O-Ti (average 121(2)°) and Ti-O-Ti (average 122.2(9)°) angles, which are clearly narrower than those observed in the previous complexes, but similar to those with an adamantane-like structure.[5a,13]

DFT elucidation of the reaction mechanism: To investigate the incorporation of the silanols to the organometallic oxides $[\{Ti(\eta^5\text{-}C_5Me_5)(\mu\text{-}O)\}_3(\mu_3\text{-}CR)]$ (R = H (**1**), Me (**2**)) at a mechanistic level, density functional theory (DFT) calculations[14] were carried out on the simplest silanol substrate, H_3SiOH, and the model complex $[\{Ti(\eta^5\text{-}C_5H_5)(\mu\text{-}O)\}_3(\mu_3\text{-}CMe)]$ (**2H**).

For **2H,** we initially analyzed the hydron-transfer process at both the alkylidyne carbon and the oxo sites. Calculations show that hydronation at the oxo site is energetically favored compared to that at the alkylidyne carbon atom by 18 kJ mol^{-1}. Therefore it is reasonable to assume that the reaction will start with the hydron transfer from the silanol to a more basic and less crowded oxo group of the organotitanium complex **2H**. Figure 5 shows the two mechanisms studied. The silanol first approaches one of the oxo groups of complex **2H,** forming the adduct **B** by SiO–H···O hydrogen bonding. The subsequent hydron transfer to the oxygen atom is accompanied by formation of the siloxide group, through a transition state $\mathbf{TS_{BC}}$, to give **C**. The computed energy barrier for the step from **B** to **C** is calculated to be relatively low, 42 kJ mol^{-1}.

As the H_3SiO fragment interacts with the titanium center in $\mathbf{TS_{BC}}$, the C_{apical}–Ti_1 bond length is elongated from 2.09 Å in **2H** to 2.34 Å in $\mathbf{TS_{BC}}$.[15a] In the intermediate **C**, the C_{apical}–Ti_1 bond is broken (2.79 Å), and the sp^3 tetrahedral environment of the carbon atom becomes closer to sp^2 planar (Ti2-Ti3-C_{apical}–C **2H**: 137.4°; **C**: 161.0°). On going from **2H** to **C**, we also observed that the energy of the HOMO, which is mainly formed by a bonding combination of p orbitals of the bridging carbon atom and d orbitals of the Ti atoms, rises significantly from −6.2 to −5.5 eV. This suggests an increase of the basicity of the bridging carbon atom.

Once complex **C** is formed, there are two plausible reaction mechanisms. First, the hydron at the oxo group could

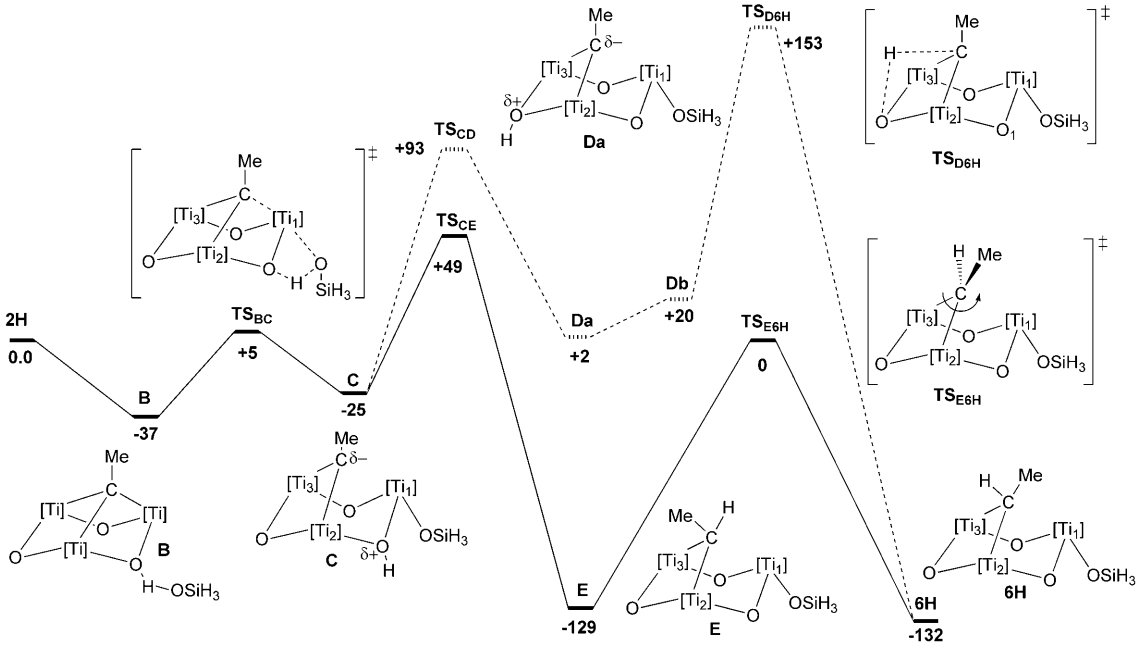

Figure 5. Potential energy profile (kJ mol^{-1}) for the incorporation of H_3SiOH to [{Ti(η^5-C_5H_5)(μ-O)}$_3$(μ_3-CMe)] (**2H**). [Ti] = Ti(η^5-C_5H_5).

migrate to the oxygen opposite the titanium silanoxide moiety to lead to complex **Da** (Scheme 4 and dashed lines in Figure 5). The energy barrier (**TS$_{CD}$**) for the step from **C** to **Da** is calculated to be 118 kJ mol^{-1}. The **Da** intermediate can rearrange to **Db** by inversion of the hydronated oxy center, leading to a more suitable disposition of the hydrogen atom for a subsequent migration to the bridging carbon to yield **6H**. However, the computed relative energy of the transition-state structure **TS$_{D6H}$** with respect to the reactants (153 kJ mol^{-1}) seems to be too high for this reaction, which occurs experimentally at room temperature.

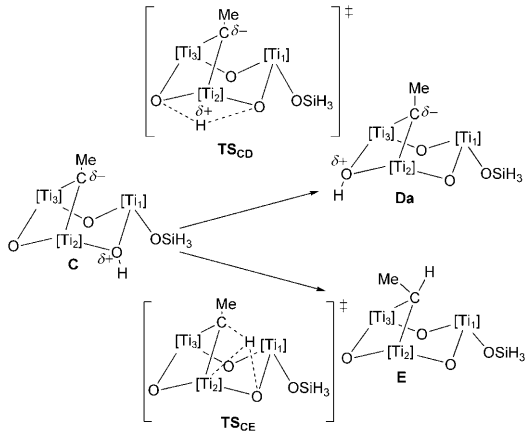

Scheme 4. [Ti] = Ti(η^5-C_5H_5).

In the other possible mechanism (Scheme 4 and solid lines in Figure 5), the hydrogen atom could directly migrate from the oxygen atom in **C** to the hydrocarbon moiety to form **E**. The energy cost to reach **TS$_{CE}$** from **C** is a modest 74 kJ mol^{-1}, which is lower than the energy cost to reach **TS$_{CD}$**. In **TS$_{CE}$** the calculated Ti_2–H distance is 1.88 Å, indicating that the titanium center may play an active role.[15b] Moreover, the intermediate **E** is much more stable than **Da** (131 kJ mol^{-1}), in accordance with the increasing basicity of the bridging carbon in **C**. The methyl substituent of the alkylidene group in **E** is oriented towards the most crowded space, between two of the three cyclopentadienyl rings. To be in agreement with the experimental findings (see Figure 1), the proposed mechanism must involve the rotation of the μ-alkylidene ligand. The computed rotational barrier on the simplified molecular model using η^5-C_5H_5 ligands amounts to 129 kJ mol^{-1} for the μ-ethylidene ligand. To analyze the potential importance of the steric effects of the pentamethylcyclopentadienyl groups, we performed additional quantum mechanics/molecular mechanics (ONIOM) calculations on the more realistic [{Ti(η^5-C_5Me_5)-(μ-O)}$_3$(μ_3-CMe)] system. Upon introduction of the steric effects, we observed that the alkylidene rotational barrier lowers significantly from 129 to 102 kJ mol^{-1}, and that the relative destabilization of the intermediate **E** with respect to the final product rises from 3 to 22 kJ mol^{-1}. These new computed values are in better agreement with the experimental observations.

The thermal μ-alkylidene carbon rotation has been observed for several transition metals, but its mechanism has remained speculative.[16] Unlike previous works, we propose a direct μ-alkylidene rotation. Figure 6 shows the molecular orbitals (MOs) involved in the μ-alkylidene rotation. In the intermediate **E**, we can dissect the bonding between the tetrahedral alkylidene carbon atom and the titanium atoms into two doubly occupied canonical MOs, which represent

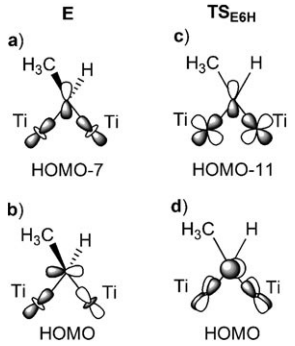

Figure 6. Schematic molecular orbitals representing the interactions between the μ-alkylidene carbon and the Ti2 and Ti3 metal centres for the intermediate **E** (a, b) and the transition state **TS$_{E6H}$** (c, d). The corresponding DFT-derived 3D molecular orbital representations are provided in the Supporting Information (Figure S4).

the two carbon–titanium σ interactions (Figure 6a,b). At the transition state **TS$_{E6H}$** we recognize one σ- and one π-type interaction between the planar alkylidene carbon and the two titanium atoms (Figure 6c,d, respectively). The stabilizing π-type interaction is viable because the two titanium centers have an available combination of empty d orbitals with appropriate symmetry to overlap with the filled p orbitals perpendicular carbon orbital (Figure 6d).

Conclusion

In summary, we have established simple and high-yield reactions to obtain titanasiloxanes derived from the organometallic oxides [{Ti(η^5-C$_5$Me$_5$)(μ-O)}$_3$(μ$_3$-CR)] (R = H (**1**), Me (**2**)) and discrete silanols such as triorganosilanols R$_3$Si(OH), silanediols R$_2$Si(OH)$_2$, or the silanetriol *t*BuSi(OH)$_3$. The synthetic strategies in all cases involved hydron-transfer processes between the silanol and μ$_3$-alkylidyne species. The novel synthesized titanasiloxanes exhibit different framework structures containing the structural unit {[Ti(η^5-C$_5$Me$_5$)O]$_3$}. DFT calculations have allowed us to describe the incorporation of the silanols at a mechanistic level. The proposal initially suggests a hydron transfer from the silanols to one oxygen atom of the Ti$_3$O$_3$ ring, followed by an intramolecular hydronation of the alkylidyne moiety. Finally, and for the first time to our knowledge, we provide theoretical evidence of a μ-alkylidene ligand rotation, which leads to the experimentally observed product.

Experimental Section

All work was performed under anaerobic and anhydrous conditions by using Schlenk-line and glovebox techniques. Solvents were carefully dried from the appropriate drying agents and distilled prior to use. Ph$_3$SiOH, *i*Pr$_3$SiOH, and Ph$_2$Si(OH)$_2$ were purchased from Aldrich and sublimed or dried/distilled before use. [{Ti(η^5-C$_5$Me$_5$)(μ-O)}$_3$(μ$_3$-CR)] (R = H (**1**), Me (**2**))[6] and *t*BuSi(OH)$_3$[17] were synthesized according to the published procedures. *i*Pr$_2$Si(OH)$_2$ was prepared by a slightly modified literature procedure.[17] Elemental analyses (C, H, N) were performed with a Heraeus CHN-O-RAPID. NMR spectra were recorded on Varian NMR system spectrometers: Unity-300 or Mercury-VX, and infrared spectra were acquired for samples in KBr pellets on a FT-IR Perkin–Elmer SPECTRUM 2000 spectrophotometer.

Synthesis of [{Ti(η^5-C$_5$Me$_5$)(μ-O)}$_3$(μ-CH$_2$)(OSiPh$_3$)] (3): A solution of **1** (0.30 g, 0.49 mmol) in hexane (40 mL) and Ph$_3$SiOH (0.14 g, 0.50 mmol) were placed in a 100 mL Schlenk flask. The reaction mixture was stirred in a glovebox at room temperature overnight. Then the orange-reddish solution was filtered, concentrated, and cooled to −20 °C to afford **3** as an orange microcrystalline solid (0.40 g, 92 %). ^{1}H NMR (300 MHz, [D$_6$]benzene, 25 °C, TMS): δ = 1.94 (s, 30 H; C$_5$*Me*$_5$), 1.98 (s, 15 H; C$_5$*Me*$_5$), 5.59, 6.32 (AB spin system, $^2J_{HH}$ = 9.3 Hz, 2 H; μ-C*H*$_2$), 7.2–8.0 ppm (m, 15 H; *Ph*$_3$SiO); ^{13}C NMR (75 MHz, [D$_6$]benzene, 25 °C, TMS): δ = 11.7, 12.0 (q, J_{CH} = 125.5 Hz, C$_5$*Me*$_5$), 120.9, 123.8 (m, *C*$_5$Me$_5$), 126.0–140.0 (*Ph*$_3$SiO), 189.7 (t, J_{CH} = 124.8 Hz, μ-*C*H$_2$); IR (KBr,): $\tilde{\nu}$ = 2910 (s), 2854 (m), 1588 (w), 1485 (w), 1427 (s), 1374 (m), 1260 (m), 1113 (s), 1029 (m), 973 (vs), 751 (vs), 708 (vs), 669 (s), 626 (s), 550 (m), 509 (s), 456 (m), 395 cm^{-1} (m); EI mass spectrum: *m/z* (%): 462 (10) [*M*−Ph$_3$SiO−CH$_2$−C$_5$Me$_5$]$^+$; elemental analysis calcd (%) for C$_{49}$H$_{62}$O$_4$SiTi$_3$ (886.71): C 66.37, H 7.05; found: C 66.39, H 7.20.

Synthesis of [{Ti(η^5-C$_5$Me$_5$)(μ-O)}$_3$(μ-CH$_2$)(OSi*i*Pr$_3$)] (4): In a similar way to **3**, compound **1** (0.30 g, 0.49 mmol) and *i*Pr$_3$SiOH (0.062 mL, 0.49 mmol) were dissolved in hexane (50 mL) and the reaction mixture was stirred overnight. After filtration, concentration (≈20 mL), and crystallization at −20 °C, complex **4** was isolated as dark red crystals (0.28 g, 71 %). ^{1}H NMR (300 MHz, [D$_6$]benzene, 25 °C, TMS): δ = 1.10–1.25 (m, (Me$_2$C*H*)$_3$SiO), 1.24 (d, $^3J_{HH}$ = 5.7 Hz, 18 H; (*Me*$_2$CH)$_3$SiO), 1.99 (s, 30 H; C$_5$*Me*$_5$), 2.06 (s, 15 H; C$_5$*Me*$_5$), 5.51, 6.27 ppm (AB spin system, 2 H; $^2J_{HH}$ = 9.3 Hz, μ-C*H*$_2$); ^{13}C NMR (75 MHz, [D$_6$]benzene, 25 °C, TMS): δ = 11.8, 12.1 (q, J_{CH} = 125.8 Hz, C$_5$*Me*$_5$), 15.3 (d, J_{CH} = 135.0 Hz, (Me$_2$*C*H)$_3$SiO), 19.1 (q, J_{CH} = 125.2 Hz, (*Me*$_2$CH)$_3$SiO), 127.7, 128.0 (m, *C*$_5$Me$_5$), 189.7 ppm (t, J_{CH} = 125.8 Hz, μ-*C*H$_2$); IR (KBr): $\tilde{\nu}$ = 2911 (s), 2860 (s), 1460 (m), 1375 (m), 1025 (w), 941 (vs), 882 (m), 738 (vs), 670 (s), 624 (m), 553 (w), 421 (w), 388 cm^{-1} (w); EI mass spectrum: *m/z* (%): 785 (1) [*M*]$^+$, 650 (45) [*M*−C$_5$Me$_5$]$^+$, 635 (1) [*M*−C$_5$Me$_5$−CH$_2$]$^+$, 592 (3) [*M*−C$_5$Me$_5$−CH$_2$−*i*Pr]$^+$, 564 (2) [*M*−C$_5$Me$_5$−CH$_2$−*i*PrSi]$^+$; elemental analysis calcd (%) for C$_{40}$H$_{68}$O$_4$SiTi$_3$ (784.66): C 61.22, H 8.73; found: C 60.79, H 8.17.

Synthesis of [{Ti(η^5-C$_5$Me$_5$)(μ-O)}$_3$(μ-CHMe)(OSiPh$_3$)] (5): Compound **2** (0.30 g, 0.48 mmol) and Ph$_3$SiOH (0.13 g, 0.48 mmol) were dissolved in hexane (40 mL) and put in a 100 mL Schlenk flask. The reaction mixture was stirred at room temperature overnight, filtered, and concentrated (≈20 mL), to afford **5** as a pale violet crystalline solid (0.41 g, 94 %). ^{1}H NMR (300 MHz, [D$_6$]benzene, 25 °C, TMS): δ = 1.89 (s, 30 H; C$_5$*Me*$_5$), 1.94 (d, $^3J_{HH}$ = 8.1 Hz, 3 H; μ-CH*Me*), 2.01 (s, 15 H; C$_5$*Me*$_5$), 6.07 (q, $^3J_{HH}$ = 7.8 Hz, 1 H; μ-C*H*Me), 7.2–8.0 ppm (m, 15 H; *Ph*$_3$SiO); ^{13}C NMR (75 MHz, [D$_6$]benzene, 25 °C, TMS): δ = 11.3, 12.3 (q, J_{CH} = 125.7 Hz, C$_5$*Me*$_5$), 29.9 (q, J_{CH} = 125.0 Hz, μ-CH*Me*), 120.3, 123.5 (m, C$_5$*Me*$_5$), 126.0–140.0 (*Ph*$_3$SiO), 207.4 ppm (d, J_{CH} = 116.5 Hz, μ-*C*HMe); IR (KBr): $\tilde{\nu}$ = 2910 (s), 2855 (s), 1651 (w), 1588 (w), 1487 (w), 1427 (s), 1376 (m), 1261 (m), 1110 (s), 1027 (m), 966 (s), 737 (vs), 704 (vs), 658 (s), 622 (s), 509 (s), 397 cm^{-1} (s); EI mass spectrum: *m/z* (%): 614 (2) [*M*−Ph$_3$Si−CHMe]$^+$, 598 (1) [*M*−Ph$_3$SiO−CHMe]$^+$, 438 (1) [*M*−Ph$_3$SiO−CHMe−C$_5$Me$_5$]$^+$; elemental analysis calcd (%) for C$_{50}$H$_{64}$O$_4$SiTi$_3$ (900.73): C 66.67, H 7.17; found: C 65.94, H 6.96.

Synthesis of [{Ti(η^5-C$_5$Me$_5$)(μ-O)}$_3$(μ-CHMe)(OSi*i*Pr$_3$)] (6): A hexane solution (30 mL) of **2** (0.30 g, 0.48 mmol) and *i*Pr$_3$SiOH (0.060 mL, 0.48 mmol) was placed in a 100 mL Schlenk flask. The reaction was stirred at room temperature overnight. The violet solution was then filtered, concentrated, and transferred to a −20 °C freezer, to yield dark violet crystals identified as **6** (0.38 g, 95 %). ^{1}H NMR (300 MHz, [D$_6$]benzene, 25 °C, TMS): δ = 1.10–1.25 (m, (Me$_2$C*H*)$_3$SiO), 1.24 (d, $^3J_{HH}$ = 6.0 Hz, 18 H; (*Me*$_2$CH)$_3$SiO), 1.91 (d, $^3J_{HH}$ = 7.8 Hz, 3 H; μ-CH*Me*), 1.96 (s, 30 H; C$_5$*Me*$_5$), 2.10 (s, 15 H; C$_5$*Me*$_5$), 5.95 ppm (q, $^3J_{HH}$ = 7.8 Hz, 1 H; μ-C*H*Me); ^{13}C NMR (75 MHz, [D$_6$]benzene, 25 °C, TMS): δ = 11.5, 12.3 (q, J_{CH} = 125.8 Hz, C$_5$*Me*$_5$), 16.2 (d, J_{CH} = 120.0 Hz, (Me$_2$CH)$_3$SiO), 19.3 (q, J_{CH} = 124.6 Hz, (*Me*$_2$CH)$_3$SiO), 29.6 (q, J_{CH} = 124.5 Hz, μ-CH*Me*),

119.8, 122.4 (m, C_5Me_5), 205.7 ppm (d, $J_{CH}=115.9$ Hz, μ-*C*HMe); IR (KBr): $\tilde{\nu}=2911$(s), 2862 (s), 1492 (w), 1437 (m), 1375 (m), 1260 (w), 1025 (w), 936 (s), 779 (vs), 732 (s), 656 (s), 621 (m), 419 cm^{-1} (m); EI mass spectrum: *m/z* (%): 771 (1) $[M-C_2H_4]^+$, 613 (3) $[M-iPr_3Si-C_2H_4]^+$; elemental analysis calcd (%) for $C_{41}H_{70}O_4SiTi_3$ (798.69): C 61.65, H 8.83; found: C 61.86, H 8.36.

Synthesis of [{Ti(η⁵-C_5Me_5)(μ-O)}$_3$(μ-O_2SiPh_2)(Me)] (7): The preparation was similar to that for **6**, but with **1** (0.30 g, 0.49 mmol), hexane (50 mL), and $Ph_2Si(OH)_2$ (0.11 g, 0.49 mmol) to give **7** (0.25 g, 61%) as a bright yellow microcrystalline solid. ^{1}H NMR (300 MHz, [D$_6$]benzene, 25°C, TMS): $\delta=0.50$ (s, 3H; Ti*Me*), 1.78 (s, 15H; C_5Me_5), 2.02 (s, 30H; C_5Me_5), 7.2–8.0 ppm (10H; Ph_2SiO_2); ^{13}C{^{1}H} NMR (75 MHz, [D$_6$]benzene, 25°C, TMS): $\delta=11.4$, 11.6 (C_5Me_5), 40.8 (Ti*Me*), 121.8, 123.9 (C_5Me_5), 126.0–152.1 ppm (Ph_2SiO_2); IR (KBr): $\tilde{\nu}=2915$ (m), 2851 (m), 1428 (s), 1376 (m), 1262 (w), 1121 (m), 1029 (w), 909 (vs), 775 (vs), 715 (vs), 604 (w), 573 (w), 505 (m), 481 (m), 417 (s), 396 cm^{-1} (s); EI mass spectrum: *m/z* (%): 811 (1) $[M-Me]^+$, 676 (3) $[M-Me-C_5Me_5]^+$, 597 (7) $[M-Me-Ph_2SiO_2]^+$, 541 (2) $[M-Me-2C_5Me_5]^+$, 462 (25) $[M-Me-Ph_2SiO_2-C_5Me_5]^+$, 406 (13) $[M-Me-3C_5Me_5]^+$, 327 (16) $[M-Me-Ph_2SiO_2-2C_5Me_5]^+$; elemental analysis calcd (%) for $C_{43}H_{58}O_5SiTi_3$ (826.61): C 62.47, H 7.07; found: C 61.93, H 7.09.

Synthesis of [{Ti(η⁵-C_5Me_5)(μ-O)}$_3$(μ-O_2Si*i*Pr_2)(Me)] (8): *i*$Pr_2Si(OH)_2$ (0.10 g, 0.67 mmol) was added to a solution of **1** (0.40 g, 0.65 mmol) in hexane (50 mL). After the reaction mixture had been stirred at room temperature overnight, it was filtered, concentrated, and cooled to −20°C to afford **8** as dark yellow crystals (0.42 g, 85%). ^{1}H NMR (300 MHz, [D$_6$]benzene, 25°C, TMS): $\delta=0.49$ (s, 3H; Ti*Me*), 0.92–1.06 (m, Me_2CHSi), 1.08–1.20 (m, Me_2CHSi), 1.23 (d, $^3J_{HH}=6.3$ Hz, 6H; Me_2CHSi), 1.31 (d, $^3J_{HH}=7.5$ Hz, 6H; Me_2CHSi), 1.96 (s, 15H; C_5Me_5), 2.02 ppm (s, 30H; C_5Me_5); ^{13}C NMR (75 MHz, [D$_6$]benzene, 25°C, TMS): $\delta=11.5$, 11.6 (q, $J_{CH}=126.4$ Hz, C_5Me_5), 14.2–16.4 (overlapped signals, Me_2CHSi), 18.3, 18.6 (q, $J_{CH}=124.2$ Hz, Me_2CHSi), 42.0 (q, $J_{CH}=121.5$ Hz, Ti*Me*), 121.3, 123.2 (m, C_5Me_5); IR (KBr): $\tilde{\nu}=2911$ (m), 2858 (m), 1458 (s), 1374 (m), 1242 (w), 1199 (m), 1071 (w), 911 (vs), 893 (vs), 759 (vs), 706 (vs), 604 (w), 564 (w), 512 (m), 467 (m), 443 (s), 393 cm^{-1} (s); EI mass spectrum: *m/z* (%) 758 (1) $[M]^+$, 743 (26) $[M-Me]^+$, 700 (3) $[M-Me-iPr]^+$, 608 (3) $[M-Me-C_5Me_5]^+$, 565 (12) $[M-Me-C_5Me_5-iPr]^+$, 522 (4) $[M-Me-C_5Me_5-2iPr]^+$; elemental analysis calcd (%) for $C_{37}H_{62}O_5SiTi_3$ (758.59): C 58.58, H 8.24; found: C 59.00, H 7.98.

Synthesis of [{Ti(η⁵-C_5Me_5)(μ-O)}$_3$(μ-O_2SiPh_2)(Et)] (9): $Ph_2Si(OH)_2$ (0.18 g, 0.66 mmol) was added to a solution of **2** (0.40 g, 0.64 mmol) in hexane (50 mL), and the resulting mixture was stirred for 4 h at room temperature. Then the solution was filtered, concentrated, and cooled to −20°C to yield **9** (0.36 g, 63%) as a pale yellow microcrystalline solid. ^{1}H NMR (300 MHz, [D$_6$]benzene, 25°C, TMS): $\delta=1.05$ (q, $^3J_{HH}=7.8$ Hz, 2H; Me*CH*$_2$Ti), 1.71 (t, $^3J_{HH}=7.8$ Hz, 3H; *Me*CH$_2$Ti), 1.78 (s, 15H; C_5Me_5), 2.03 (s, 30H; C_5Me_5), 7.2–8.0 ppm (m, 10H; Ph_2SiO_2); ^{13}C NMR (75 MHz, [D$_6$]benzene, 25°C, TMS): $\delta=11.0$, 11.4 (q, $J_{CH}=125.1$ Hz, C_5Me_5), 17.9 (q, $J_{CH}=123.2$ Hz, *Me*CH$_2$Ti), 58.1 (t, $J_{CH}=120.8$ Hz, Me*CH*$_2$Ti), 121.2, 123.5 (m, C_5Me_5), 127.1–140.7 ppm (Ph_2SiO_2); IR (KBr): $\tilde{\nu}=2909$ (m), 1590 (w), 1428 (m), 1375 (m), 1262 (w), 1120 (m), 1029 (w), 908 (vs), 770 (vs), 712 (vs), 627 (w), 601 (w), 572 (m), 506 (m), 482 (m), 414 cm^{-1} (m); EI mass spectrum: *m/z* (%): 812 (2) $[M-C_2H_5]^+$, 598 (7) $[M-C_2H_5-Ph_2SiO_2]^+$; elemental analysis calcd (%) for $C_{44}H_{60}O_5SiTi_3$ (840.65): C 62.86, H 7.19; found: C 63.07, H 6.90.

Synthesis of [{Ti(η⁵-C_5Me_5)(μ-O)}$_3$(μ-O_2Si*i*Pr_2)(Et)] (10): The procedure described for complex **9** was used, but with *i*$Pr_2Si(OH)_2$ (0.10 g, 0.67 mmol) and **2** (0.40 g, 0.64 mmol) in hexane (50 mL). Complex **10** was isolated as a dark yellow crystalline solid (0.45 g, 92%). ^{1}H NMR (300 MHz, [D$_6$]benzene, 25°C, TMS): $\delta=0.96$–1.14 (m, 2H; Me_2CHSi) overlapping with 1.08 (q, $^3J_{HH}=7.5$ Hz, 2H; Me*CH*$_2$Ti), 1.24 (d, $^3J_{HH}=6.3$ Hz, 6H; Me_2CHSi), 1.33 (d, $^3J_{HH}=7.2$ Hz, 6H; Me_2CHSi), 1.65 (t, $^3J_{HH}=7.5$ Hz, 3H; *Me*CH$_2$Ti), 1.97 (s, 15H; C_5Me_5), 2.04 ppm (s, 30H; C_5Me_5); ^{13}C NMR (75 MHz, [D$_6$]benzene, 25°C, TMS): $\delta=11.6$, 11.7 (q, $J_{CH}=125.7$ Hz, C_5Me_5), 15.4, 16.0 (d, $J_{CH}=112.8$ Hz, Me_2CHSi), 17.8 (q, $J_{CH}=123.2$ Hz, *Me*CH$_2$Ti), 18.1, 18.9 (q, $J_{CH}=124.5$ Hz, Me_2CHSi), 57.4 (t, $J_{CH}=119.6$ Hz, Me*CH*$_2$Ti), 121.2, 123.2 ppm (m, C_5Me_5); IR (KBr): $\tilde{\nu}=2912$ (m), 2862 (m), 1494 (w), 1445 (m), 1374 (m), 1239 (w), 1070 (w), 892 (vs), 760 (vs), 701 (vs), 624 (w), 509 (m), 467 (m), 411 cm^{-1} (m); EI mass spectrum: *m/z* (%): 743 (10) $[M-C_2H_5]^+$, 700 (2) $[M-C_2H_5-iPr]^+$, 565 (9) $[M-C_2H_5-iPr-C_5Me_5]^+$, 522 (2) $[M-C_2H_5-2iPr-C_5Me_5]^+$, 430 (10) $[M-C_2H_5-2iPr-2C_5Me_5]^+$; elemental analysis calcd (%) for $C_{38}H_{64}O_5SiTi_3$ (772.62): C 59.07, H 8.35; found: C 59.23, H 8.22.

Synthesis of [{Ti(η⁵-C_5Me_5)(μ-O)}$_3$(μ-O_2Si(OH)*t*Bu)(Me)] (11): *t*Bu(OH)$_3$ (5.00 mg, 0.03 mmol) and **1** (20.00 mg, 0.03 mmol) were placed in an amber-stained NMR tube with a Young valve and dissolved in C_6D_6 (0.6 mL). After eight hours, the reaction was checked by ^{1}H and ^{13}C NMR spectroscopy allowing detection and characterization of compound **11**, slightly contaminated (≈10%) with **13**. ^{1}H NMR (300 MHz, [D$_6$]benzene, 25°C, TMS): $\delta=0.48$(s, 3H; C*H*$_3$), 1.29 (s, 9H; *t*BuSi), 1.99 (s, 15H; C_5Me_5), 2.02 ppm (s, 30H; C_5Me_5); ^{13}C NMR (75 MHz, [D$_6$]benzene, 25°C, TMS): $\delta=11.6$, 11.6 (q, $J_{CH}=126.4$ Hz, C_5Me_5 overlapping), 18.4 (br s, Me_3CSi), 27.5 (qm, $J_{CH}=123.9$ Hz, Me_3CSi), 41.6 (q, $J_{CH}=120.7$ Hz, Ti*CH*$_3$), 121.8, 123.6 ppm (m, C_5Me_5); the SiOH ^{1}H NMR signal could not be unambiguously assigned.

Synthesis of [{Ti(η⁵-C_5Me_5)(μ-O)}$_3$(μ-O_2Si(OH)*t*Bu)(Et)] (12): **2** (0.40 g, 0.64 mmol), *t*BuSi(OH)$_3$ (0.09 g,0.64 mmol) and hexane (40 mL) were placed in an amber-stained 100 mL Carious tube. The reaction mixture was stirred at room temperature overnight. The resulting solution was filtered, concentrated, and cooled to −20°C, to afford **12** as yellow crystals in 73% (0.36 g) yield. ^{1}H NMR (300 MHz, [D$_6$]benzene, 25°C, TMS): $\delta=$ 0.99 (q, 2H; $^3J_{HH}=7.5$ Hz, MeC*H*$_2$Ti), 1.28 (s, 9H; *t*BuSi), 1.69 (t, 3H; $^3J_{HH}=7.5$ Hz, *Me*CH$_2$Ti), 1.95 (s, 15H; C_5Me_5), 2.00 (s, 1H; SiOH), 2.04 ppm (s, 30H; C_5Me_5); ^{13}C NMR (75 MHz, [D$_6$]benzene, 25°C, TMS):=11.4, 11.5 (q, $J_{CH}=126.4$ Hz, C_5Me_5), 18.0 (br s, Me_3CSi), 18.4 (q, $J_{CH}=123.3$ Hz, *Me*CH$_2$Ti), 28.0 (qm, $J_{CH}=124.5$ Hz, Me_3CSi), 58.7 (tm, $J_{CH}=125.5$ Hz, Me*CH*$_2$Ti), 121.4, 123.6 ppm (m, C_5Me_5); IR (KBr): $\tilde{\nu}=$ 3645(w), 2914 (m), 2852 (m), 1474 (w), 1460 (m), 1375 (m), 896 (vs), 769 (vs), 715 (vs), 627 (w), 600 (w), 555 (m), 528(w), 469 (s), 420 cm^{-1} (s); EI mass spectrum: *m/z* (%): 731 (3) $[M-C_2H_5]^+$, 598 (2) $[M-C_2H_5-tBuSiO_3]^+$; elemental analysis calcd (%) for $C_{36}H_{60}O_6SiTi_3$ (760.56): C 56.85, H 7.95; found: C 56.94, H 7.63.

Synthesis of [{Ti(η⁵-C_5Me_5)(μ-O)}$_3$(μ-O_3Si*t*Bu)] (13): A solution of **2** (0.50 g, 0.80 mmol) and *t*BuSi(OH)$_3$ (0.11 g, 0.80 mmol) in toluene (40 mL) was heated for three days at 100°C with stirring. Then the solution was filtered, concentrated, and cooled to −20°C to yield yellow crystals identified as **13** in a yield of 86% (0.50 g). ^{1}H NMR (300 MHz, [D$_6$]benzene, 25°C, TMS): $\delta=1.24$ (s, 9H; *t*BuSi), 2.04 ppm (s, 45H; C_5Me_5); ^{13}C NMR (75 MHz, [D$_6$]benzene, 25°C, TMS): $\delta=11.4$ (q, $J_{CH}=$ 126.3 Hz, C_5Me_5), 17.8 (bs, Me_3CSi), 27.1 (qm, $J_{CH}=124.5$ Hz, Me_3CSi), 123.0 ppm (m, C_5Me_5); IR (KBr): $\tilde{\nu}=2949$ (m), 2915 (m), 2850 (m), 1496 (w), 1471 (m), 1458 (m), 1375 (m), 1262 (w), 1056 (w), 1009 (w), 899 (vs), 875 (vs), 776 (s), 697 (vs), 601 (m), 570 (s), 431 (s), 408 (s), 377 cm^{-1} (s); elemental analysis calcd (%) for $C_{34}H_{54}O_6SiTi_3$ (730.49): C 55.90, H 7.45; found: C 55.69, H 7.31.

X-ray structure analyses of 6, 10, 12, and 13: Crystals of complexes **6**, **10**, **12**, and **13** were grown from saturated hexane solutions at −20°C, removed from the Schlenks and covered with a layer of a viscous perfluoropolyether (Fomblin®Y). A suitable crystal was selected with the aid of a microscope, attached to a glass fiber, and immediately placed in the low-temperature nitrogen stream of the diffractometer. The intensity data sets were collected at 200 K on a Bruker-Nonius KappaCCD diffractometer equipped with an Oxford Cryostream 700 unit. Crystallographic data for all the complexes are presented in Table 1. The structures were solved using the WINGX package[18] by direct methods (SHELXS-97), and refined by least-squares against F^2 (SHELXL-97).[19]

Complex **6** showed disorder in the C21–C30 pentamethylcyclopentadienyl group; two different positions were refined with 51.5 and 48.5% occupancy, respectively. All non-hydrogen atoms of **6**, except C30′, were anisotropically refined. The hydrogen atoms were positioned geometrically and refined by using a riding model, and the ethylidene hydrogen atoms were located in the Fourier difference map and isotropically refined.

Complex **10** was studied with the $P2_1/c$ space group. After the solution and refinement we found a situation of merohedral twining using the

Table 1. Crystal data and structure refinement for **6**, **10**, **12**, and **13**.

Compound	**6**	**10**	**12**	**13**
formula	$C_{41}H_{70}O_4SiTi_3$	$C_{38}H_{64}O_5SiTi_3$	$C_{36}H_{60}O_6SiTi_3$	$C_{34}H_{54}O_6SiTi_3$
M_r	798.76	772.68	760.63	730.56
T [K]	200(2)	200(2)	200(2)	200(2)
λ ($Mo_{K\alpha}$) [Å]	0.71073	0.71073	0.71073	0.71073
crystal system	monoclinic	monoclinic	orthorhombic	monoclinic
space group	$P2_1/n$	$P2_1/c$	*Pnma*	*C*2
a [Å]	19.598(5)	16.674(4)	19.254(4)	19.300(5)
b [Å]	11.1026(11)	16.408(4)	16.546(4)	19.186(4)
c [Å]	21.337(7)	15.859(5)	12.7762(14)	11.2989(16)
β [°]	102.27(2)°	90.30(2)°		109.182(13)°
V [Å^3]	4536.7(19)	4339(2)	4070.2(13)	3951.4(14)
Z	4	4	4	4
ρ_{calcd} [g cm^{-3}]	1.169	1.183	1.241	1.228
μ ($Mo_{K\alpha}$) [mm^{-1}]	0.576	0.602	0.642	0.659
F(000)	1712	1648	1616	1544
crystal size [mm^3]	0.21×0.20×0.11	0.47×0.42×0.35	0.10×0.10×0.10	0.36×0.25×0.21
θ range	3.03 to 27.50°	5.05 to 27.71°	3.12 to 27.51°	3.08 to 27.52°
index ranges	$-25\le h\le 25$	$-21\le h\le 21$	$-24\le h\le 24$	$-25\le h\le 25$,
	$-14\le k\le 14$	$-21\le k\le 21$	$-21\le k\le 21$	$-24\le k\le 24$
	$-27\le l\le 27$	$-20\le l\le 20$	$-16\le l\le 16$	$-14\le l\le 14$
collected reflns	91485	87838	88592	74981
independent reflns	10419	9966	4824	9094
	[R(int) = 0.127]	[R(int) = 0.083]	[R(int) = 0.107]	[R(int) = 0.065]
GOF	1.025	1.136	1.010	1.037
final R indices [$F>4\sigma(F)$]	$R1 = 0.058$	$R1 = 0.062$	$R1 = 0.052$	$R1 = 0.056$
	$wR2 = 0.125$	$wR2 = 0.137$	$wR2 = 0.117$	$wR2 = 0.112$
R indices (all data)	$R1 = 0.129$	$R1 = 0.087$	$R1 = 0.109$	$R1 = 0.111$
	$wR2 = 0.146$	$wR2 = 0.145$	$wR2 = 0.140$	$wR2 = 0.128$
largest diff. peak/hole [e Å^{-3}]	0.815/−0.855	0.540/−0.666	0.805/−0.523	0.382/−0.324

TwinRotMat procedure of the PLATON package.[20] The optimization of the BASF parameter in the refinement showed a 34% contribution of the second component. No solvent or disorder was found in the study, and all the non-hydrogen atoms were refined anisotropically. The hydrogen atoms were positioned geometrically and refined by using a riding model.

Complex **12** showed disorder for the Si3 atom, and two different positions were refined with 90 and 10% occupancy, respectively. All non-hydrogen atoms of **12** were anisotropically refined. The hydrogen atoms were positioned geometrically and refined by using a riding model, and the hydroxyl group was located in the Fourier difference map and isotropically refined.

The crystal structure of compound **13** was studied with the *C*2*m* and *C*2 space groups. As the disorder found for the C11–C20 pentamethylcyclopentadienyl group could not be modeled with the centrosymmetric space group, the *C*2 one was finally chosen. Therefore two different sites were found and refined with 51.3 and 47.7% occupancy, respectively, for the C11–C20 moiety. All non-hydrogen atoms were anisotropically refined, except those of the disordered ligand. The hydrogen atoms were positioned geometrically and refined by using a riding model.

CCDC-670713 (**3**) -670714 (**4**), -670715 (**6**), -670716 (**8**), -670717 (**10**), -681046 (**12**), and -681047 (**13**) contain the supplementary crystallographic data for this paper. These data can be obtained free of charge from The Cambridge Crystallographic Data Centre via www.ccdc.cam.ac.uk/data_request/cif. Full details of the refinements can be found in the Supporting Information.

Computational details: Full quantum mechanics calculations on the simplest silanol substrate H_3SiOH and the model complex [{Ti(η^5-C_5H_5)(μ-O)}$_3$(μ_3-CMe)] (**2H**) were performed with the GAUSSIAN03 series of programs[21] within the framework of the density functional theory (DFT)[14] by using the B3LYP functional.[22] A quasi-relativistic effective core potential operator was used to represent the 10 innermost electrons of the Ti and Si atoms.[23] The basis set for Ti and Si atoms was that associated with the pseudopotential,[24] with a standard double-ξ LANL2DZ contraction.[21] The 6–31G(d) basis set was used for C and O atoms,[24] the 6–31G(p) basis set was used for the migrating hydron,[24] whereas the 6–31G basis set was used for the other hydrogen atoms.[24] Geometry optimizations were carried out without any symmetry restrictions, and all stationary points were optimized with analytical first derivatives. Transition states were characterized by a single imaginary frequency, the normal mode of which corresponded to the expected motion.

To account for the steric effects of the methyl substituents of the η^5-C_5Me_5 ligands, we performed hybrid quantum mechanics/molecular mechanics (QM/MM) calculations, using the ONIOM method[25] as implemented in the GAUSSIAN 03 series of programs.[21] The QM region of the complex was [{Ti(η^5-C_5H_5)(μ-O)}$_3$(μ_3-CMe)] and the silanol, while the MM region was that constituted by the methyl substituents of the η^5-C_5Me_5 groups. The QM level was the same as described above. Molecular mechanics calculations used the UFF force field.[26]

Acknowledgements

Financial support for this work was provided by the Ministerio de Ciencia y Tecnología (CTQ2005-00238 and CTQ2005-06090-C02-01), Universidad de Alcalá-Comunidad de Madrid (CCG06-UAH/PPQ-0665), Factoría de Cristalización (CONSOLIDER-INGENIO 2010), and CIRIT of Generalitat de Catalunya (2005SGR00104). O. González-Del Moral thanks the M.E.C. for a doctoral fellowship.

[1] a) F. J. Feher, T. A. Budzichowski, *Polyhedron* **1995**, *14*, 3239–3253; b) R. Murugavel, V. Chandrasekhar, H. W. Roesky, *Acc. Chem. Res.* **1996**, *29*, 183–189; c) R. Murugavel, A. Voigt, M. G. Walawalkar, H. W. Roesky, *Chem. Rev.* **1996**, *96*, 2205–2236; d) R. Murugavel, M. Bhattacharjee, H. W. Roesky, *Appl. Organomet. Chem.* **1999**, *13*, 227–243.

[2] R. Murugavel, H. W. Roesky, *Angew. Chem.* **1997**, *109*, 491–494; *Angew. Chem. Int. Ed. Engl.* **1997**, *36*, 477–479, and references therein.

[3] See for example: a) M. C. Klunduk, T. Maschmeyer, J. M. Thomas, B. F. G. Johnson, *Chem. Eur. J.* **1999**, *5*, 1481–1485; b) M. D. Skowronska-Ptasinska, M. L. W. Vorstenbosch, R. A. van Santen, H. C. L. Abbenhuis, *Angew. Chem.* **2002**, *114*, 659–661; *Angew. Chem. Int. Ed.* **2002**, *41*, 637–639; c) R. Duchateau, *Chem. Rev.* **2002**, *102*, 3525–3542, and references therein.

[4] J. M. Thomas, G. Sankar, *Acc. Chem. Res.* **2001**, *34*, 571–581.

[5] a) A. Voigt, R. Murugavel, M. L. Montero, H. Wesel, F. Q. Liu, H. W. Roesky, I. Usón, T. Albers, E. Parisini, *Angew. Chem.* **1997**, *109*, 1020–1022; *Angew. Chem. Int. Ed. Engl.* **1997**, *36*, 1001–1003; b) R. Fandos, A. Otero, A. Rodríguez, M. J. Ruíz, P. Terreros, *Angew. Chem.* **2001**, *113*, 2968–2971; *Angew. Chem. Int. Ed.* **2001**, *40*, 2884–2887; c) R. Fandos, B. Gallego, A. Otero, A. Rodríguez, M. J. Ruíz, P. Terreros, *Dalton Trans.* **2007**, 871–877.

[6] a) R. Andrés, M. Galakhov, A. Martín, M. Mena, C. Santamaría, *Organometallics* **1994**, *13*, 2159–2163; b) R. Andrés, M. Galakhov, A. Martín, M. Mena, C. Santamaría, *J. Chem. Soc. Chem. Commun.* **1995**, 551–552.

[7] R. Andrés, M. V. Galakhov, M. P. Gómez-Sal, A. Martín, M. Mena, M. C. Morales-Varela, C. Santamaría, *Chem. Eur. J.* **2002**, *8*, 805–811, and references therein.
[8] a) G. Brieger, T. J. Nestrick. *Chem. Rev.*, **1974**, *74*, 567–580; b) R. A. W. Johnstone, A. H. Wilby, I. D. Entwistle, *Chem. Rev.* **1985**, *85*, 129–170.
[9] All the X-ray diffraction studies of complexes **3**, **4**, and **8** are included in the Supporting Information.
[10] O. González-del Moral, A. Martín, M. Mena, M. C. Morales-Varela, C. Santamaría, *Chem. Commun.* **2005**, 3682–3684.
[11] J. March, *Advanced Organic, Chemistry: Reactions, Mechanism, and Structure*, Wiley, New York, **1985**.
[12] R. Andrés, M. Galakhov, M. P. Gómez-Sal, A. Martín, M. Mena, C. Santamaría, *J. Organomet. Chem.* **1996**, *526*, 135–143, and references therein.
[13] a) L. M. Babcock, V. W. Day, W. G. Klemperer, *J. Chem. Soc. Chem. Commun.* **1987**, 858–859; b) M. P. Gómez-Sal, M. Mena, P. Royo, R. Serrano, *J. Organomet. Chem.* **1988**, *358*, 147–159.
[14] R. G. Parr, W. Yang, *Density Functional Theory of Atoms and Molecules*. Oxford University Press: Oxford, UK, **1989**; T. Ziegler, *Chem. Rev.* **1991**, *91*, 651–667.
[15] O. González-del Moral, A. Hernán-Gómez, A. Martín, M. Mena, C. Santamaría, *Dalton Trans.* **2008**, 44–46; a) A similar elongation is produced by incorporation of $AlMe(OH)_2$ with two molecules of complex **1**; b) A Ti···H distance of 1.86(5) Å is also found when complex **1** is coordinated to 9-borabicyclo[3.3.1]nonane (9-BBN).
[16] J. T. Park, M. -K. Chung, K. M. Chun, S. S. Yun, S. Kim, *Organometallics* **1992**, *11*, 3313–3319, and references therein.
[17] a) T. Takiguchi, *J. Am. Chem. Soc.* **1959**, *81*, 2359–2361; b) N. Winkhofer, H. W. Roesky, M. Noltemeyer, W. T. Robinson, *Angew. Chem.* **1992**, *104*, 670–671; *Angew. Chem. Int. Ed. Engl.* **1992**, *31*, 599–601.
[18] L. J. Farrugia, *J. Appl. Crystallogr.* **1999**, *32*, 837–838.
[19] G. M. Sheldrick, SHELX97, Program for Crystal Structure Analysis (Release 97–2). Universität Göttingen, Germany, **1998**.
[20] PLATON. A. L. Spek, *J. Appl. Crystallogr.* **2003**, *36*, 7–13.
[21] Gaussian 03 (Revision B.03), M. J. Frisch, G. W. Trucks, H. B. Schlegel, G. E. Scuseria, M. A. Robb, J. R. Cheeseman, J. A. Montgomery Jr., T. Vreven, K. N. Kudin, J. R. Burant, J. M. Millam, S. S. Iyengar, J. Tomasi, V. Barone, B. Mennucci, M. Cossi, G. Scalmani, N. Rega, G. A. Petersson, H. Nakatsuji, M. Hada, M. Ehara, K. Toyota, R. Fukuda, J. Hasegawa, M. Ishida, T. Nakajima, Y. Honda, O. Kitao, H. Nakai, M. Klene, X. Li, J. E. Knox, H. P. Hratchian, J. B. Cross, C. Adamo, J. Jaramillo, R. Gomperts, R. E. Stratmann, O. Yazyev, A. J. Austin, R. Cammi, C. Pomelli, J. W. Ochterski, P. Y. Ayala, K. Morokuma, G. A. Voth, P. Salvador, J. J. Dannenberg, V. G. Zakrzewski, S. Dapprich, A. D. Daniels, M. C. Strain, O. Farkas, D. K. Malick, A. D. Rabuck, K. Raghavachari, J. B. Foresman, J. V. Ortiz, Q. Cui, A. G. Baboul, S. Clifford, J. Cioslowski, B. B. Stefanov, G. Liu, A. Liashenko, P. Piskorz, I. Komaromi, R. L. Martin, D. J. Fox, T. Keith, M. A. Al-Laham, C. Y. Peng, A. Nanayakkara, M. Challacombe, P. M. W. Gill, B. G. Johnson, W. Chen, M. W. Wong, C. Gonzalez, J. A. Pople, Gaussian, Inc., Pittsburgh, PA, **2004**.
[22] a) C. Lee, C. Yang, R. G. Parr, *Phys. Rev. B* **1988**, *37*, 785–789; b) A. D. Becke, *J. Chem. Phys.* **1993**, *98*, 5648–5652; c) P. J. Stephens, F. J. Devlin, C. F. Chabalowski, M. J. Frisch, *J. Phys. Chem.* **1994**, *98*, 11623–11627.
[23] P. J. Hay, W. R. Wadt, *J. Chem. Phys.* **1985**, *82*, 299–310.
[24] a) M. M. Francl, W. J. Pietro, W. J. Hehre, J. S. Binkley, M. S. Gordon, D. J. Defrees, J. A. Pople, *J. Chem. Phys.* **1982**, *77*, 3654–3665; b) W. J. Hehre, R. Ditchfield, J. A. Pople, *J. Chem. Phys.* **1972**, *56*, 2257–2261; c) P. C. Hariharan, J. A. Pople, *Theor. Chim. Acta* **1973**, *28*, 213–222.
[25] a) F. Maseras, K. Morokuma, *J. Comput. Chem.* **1995**, *16*, 1170–1179; b) S. Humbel, S. Sieber, K. Morokuma, *J. Chem. Phys.* **1996**, *105*, 1959–7967; c) M. Svensson, S. Humbel, R. D. J. Froese, T. Matsubara, S. Sieber, K. Morokuma, *J. Phys. Chem.* **1996**, *100*, 19357–19363; d) M. Svensson, S. Humbel, K. Morokuma, *J. Chem. Phys.* **1996**, *105*, 3654–3661; e) S. Dapprich, I. Komáromi, K. S. Byun, K. Morokuma, M. J. Frisch, *J. Mol. Struct. THEOCHEM* **1999**, *461–462*, 1–21.
[26] A. K. Rappé, C. J. Casewit, K. S. Colwell, W. A. Goddard, III, W. M. Skiff, *J. Am. Chem. Soc.* **1992**, *114*, 10024–10035.

Received: April 3, 2008
Published online: July 9, 2008

